

SUBTLE INTERPLAY BETWEEN HYDROGEN AND MAGNETISM IN Co DOPED ZnO

Y. B. ZHANG,* M. H. N. ASSADI and S. LI

*School of Materials Science and Engineering
The University of New South Wales
Sydney, NSW 2052, Australia
y.zhang@unsw.edu.au

Received 2 September 2011
Accepted 18 February 2012
Published 11 June 2012

The effects of hydrogen, either interstitial (H_I) or substitutional (H_o), on magnetic properties of Co doped ZnO (ZnO:Co) have been systematically investigated using first-principles density functional calculations. The study discovers the correlation between the distribution of Co ions and the hydrogen point defect and magnetism. It is found that Co ions and hydrogen have a strong tendency toward aggregation and hydrogen mainly contributes to the room temperature ferromagnetism observed experimentally in ZnO:Co. Furthermore, in ZnO:Co, the formation of H_o with four-fold hydrogenic bonds is favored over H_I by 0.4 eV.

Keywords: Hydrogen; zinc oxides; magnetic semiconductors; density functional theory.

1. Introduction

Transition metal doped ZnO dilute magnetic oxides (DMO) have attracted great attention due to their potential as ideal materials for practical spintronic semiconductor devices [Pan *et al.*, 2008]. Of those, the Co doped ZnO (ZnO:Co) DMO has initiated enormous scientific interests since it satisfies two major criteria for being one of the most promising materials for semiconductor spintronics: (1) Curie temperature above room temperature and (2) existing technology for the materials in other applications. Despite tremendous works focusing on the ZnO:Co DMO [Prellier *et al.*, 2003; Chambers *et al.*, 2006], its origin of ferromagnetism has not been well understood yet. Recently a work by Walsh *et al.* predicted the stabilization of a ferromagnetic phase in ZnO:Co by electron doping [Walsh *et al.*, 2008]. However, no ferromagnetism was observed in highly conductive ZnO:Co samples [Kaspar *et al.*, 2008]. Considering the lack of an unambiguous correlation between carrier concentration and magnetism in experimental findings, ferromagnetism may

*Corresponding author.

lie in the interplay between defects in ZnO and the Co dopants [Assadi *et al.*, 2009]. As a dominant extrinsic impurity defect, unintentionally doped hydrogen is believed to occur in high concentrations in ZnO depending on the growth condition. Theoretical investigations suggest that interstitial hydrogen (H_I) enhances the magnetic properties of ZnO:Co by opening a channel for a spin-spin interaction among Co ions [Park and Chadi, 2005]. Furthermore, hydrogen in ZnO besides the interstitial site where it forms a hydrogen bond with O, can also substitute oxygen (H_O) and form multicentre bonds where a hydrogen ion bonds equally to all the surrounding Zn ions, becoming fourfold coordinated [Janotti and Van de Walle, 2007]. These motivated the researchers to systematically investigate and compare the interplay between the two hydrogen point defects, H_O and H_I , and Co dopants in the ZnO:Co DMO.

2. Methods

Total energy density functional calculations were performed using generalized gradient approximation (PW91) as implemented in CASTEP code [Segall *et al.*, 2002]. Energy cut-off and k -point mesh were set to be 800 eV and $3 \times 3 \times 1$ respectively. Lattice parameters of doped ZnO structures were fixed and all internal atomic coordinates were relaxed until the Cartesian force components were smaller than 0.05 eV/Å. To simulate doped structures, a 32-atom $2a \times 2a \times 2c$ wurtzite ZnO supercell as shown in Fig. 1 was adopted for calculations with two substitutional Co ions and one H ion, either interstitial (H_I) or substitutional (H_O). To systematically investigate the distribution pattern of Co and H ions in ZnO and its effect on magnetism, Co dopants and H were placed in different arrangement to constitute variety of complexes in each configuration. Two sets of typical configurations among many possibilities were considered in Table 1: the first set, configurations 1(a)–7(a), contained H_I as $Zn_{14}Co_2O_{16}H_I$ and the second set, configurations 1(b)–5(b), contained H_O as $Zn_{14}Co_2O_{15}H_O$.

The total energy of each configuration was calculated for ferromagnetic ($E_{Conf.No.}^{FM}$) and antiferromagnetic ($E_{Conf.No.}^{AFM}$) spin alignments of high-spin Co ions. The lower one is referred as total energy ($E_{Conf.No.}^{total}$) of every particular configuration. $\Delta E_{Conf.No.}$ is defined to be $(E_{Conf.No.}^{AFM} - E_{Conf.No.}^{FM})/2$ as an indicator of ferromagnetic phase stability. The formation energy of a complex in each configuration is defined as:

$$E_{Conf.No.}^f = E_{Conf.No.}^{total} - E_{ZnO}^{total} - \sum_i n_i \mu_i \quad (1)$$

where $E_{Conf.No.}^{total}$ and E_{ZnO}^{total} are total energy of the defective and pure ZnO supercells respectively, n_i is the number of atoms of type i (host or impurity atoms) that have been added to ($n_i > 0$) or removed from ($n_i < 0$) the supercell when the defect is created and μ_i is their corresponding chemical potential which only depends on experimental growth conditions [Van de Walle and Neugebauer, 2004]. Here, μ_{Co}

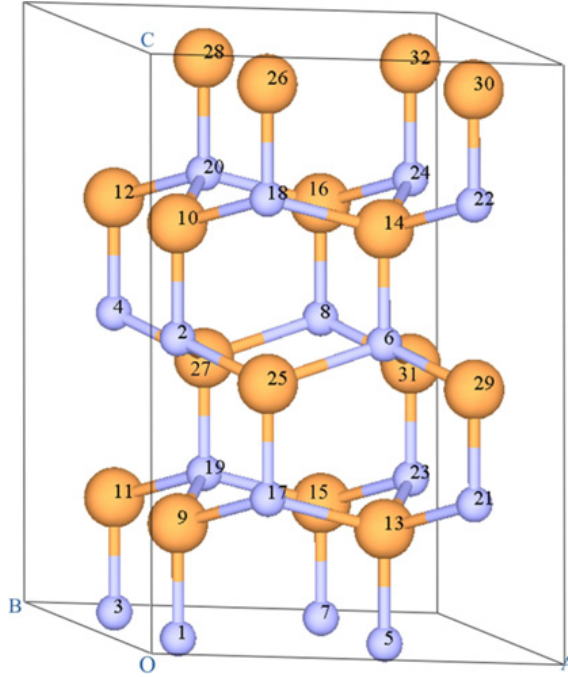


Fig. 1. A 32-atom $2 \times 2 \times 2$ ZnO supercell with lattice sites labeled. Large (small) balls represent O (Zn) ions.

Table 1. The positions of Co ions and H_I in the supercell for configurations 1(a)–7(a) or H_O for configurations 1(b)–5(b) are presented. H_I is in between two lattice sites indicated. D_{Co-Co} is the distance between Co ions and D_{near} (D_{far}) stands for the distance between the defect and the closer (further) Co ion in the relaxed structures.

Configuration Number	Type of the Defect	Position of the Defect	Positions of Co Ions	D_{Co-Co} (Å)	D_{near} (Å)	D_{far} (Å)
1(a)	H_I	20–27	17,24	6.219	3.881	4.737
2(a)	H_I	24–32	17,19	2.974	5.186	5.207
3(a)	H_I	16–20	17,19	3.087	4.950	5.356
4(a)	H_I	20–27	17,19	3.263	3.615	4.696
5(a)	H_I	20–28	6,17	3.137	5.137	5.360
6(a)	H_I	9–19	17,19	4.146	1.890	2.639
7(a)	H_I	17–25	6,17	3.539	1.780	2.401
1(b)	H_O	31	17,24	6.269	2.863	3.300
2(b)	H_O	14	17,19	3.281	5.028	6.001
3(b)	H_O	16	6,17	3.154	3.890	5.999
4(b)	H_O	9	17,19	3.079	1.738	1.738
5(b)	H_O	25	6,17	2.870	1.684	1.731

and μ_{Zn} are set to be the calculated energies of metallic Co and Zn per element respectively while μ_H is set to be half of the energy of a H_2 molecule. μ_O was calculated for oxygen-poor environments where $\mu_O = E^{total}(O_2)/2 + \Delta H^f(ZnO)$, in which $\Delta H^f(ZnO)$ is the formation enthalpy of ZnO.

3. Results and Discussions

In configuration 1(a), the Co ions are located at the most distant possible while H_I is far from them to form a scattered pattern for the distribution of Co ions and H_I. Configurations 2(a), 3(a) and 4(a) form when Co ions are paired via O within *ab* plane while H_I moves toward both Co ions by sitting on the either midbond (MB) or antibond (AB) position of a Zn-O bond [Van de Walle, 2000]. In configuration 5(a), Co ions are paired via O along *c* direction while H_I is positioned on the MB of a Zn-O bond as far as possible from both Co ions. In configurations 6(a) and 7(a), H_I sits on the MB position of a Co-O bond with the closest separation possible to a Co pair within *ab* plane and along *c* direction respectively. Like the case in ZnO:Co [Zhang *et al.*, 2009], Co's tendency toward aggregation is also observed in the presence of H_I since configuration 1(a) with the most scattered complex stands as the least stable with $E_{1(a)}^f$ of 3.01 eV as shown in Fig. 2. When Co ions are located closer, it decreases with $E_{2(a)}^f$, $E_{3(a)}^f$, $E_{4(a)}^f$ and $E_{5(a)}^f$ of 2.62 eV, 2.77 eV, 2.61 eV and 2.71 eV respectively. The great stabilization is observed in configurations 6(a) and 7(a) with $E_{6(a)}^f$ and $E_{7(a)}^f$ being 1.51 eV and 2.03 eV respectively, indicating that configuration 6(a) is the most stabilized one. In thermodynamic equilibrium, the concentration *c* of a complex is proportional to $N \exp(-E^f/k_B T)$ where *N* is the number of realizations of the complex in the supercell, E^f is the complex formation energy, k_B is Boltzmann's constant and *T* is temperature [Van de Walle and Neugebauer, 2004]. The relative concentration of the first and second most stable complexes ($c_{6(a)}/c_{7(a)}$) is 7.6×10^{12} , indicating that the Co-H_I-O-Co complex within *ab* plane is dominant and formation of the less stabilized complex is unlikely in the ZnO supercell.

In configuration 1(a), the stabilization of ferromagnetic phase is reasonably high enough to achieve the room temperature ferromagnetism as $\Delta E_{1(a)}$ equals to 86.8 meV/Co as shown in Fig. 2. However, as aforementioned, the Co dopants

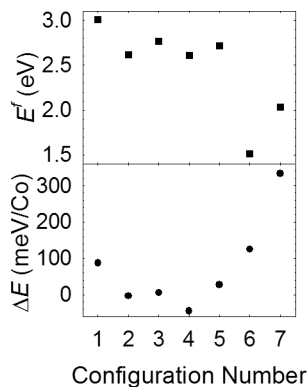


Fig. 2. (Top) Formation energy, $E_{\text{Conf.No.}}^f$ and (Bottom) difference in total energy between AFM and FM, $\Delta E_{\text{Conf.No.}}$ in configurations 1(a)–7(a) for $\text{Zn}_{14}\text{Co}_2\text{O}_{16}\text{H}_I$.

and the H_I defect are unlikely to be arranged in this scattered pattern with thermodynamic equilibrium. By moving to more compact complexes as in configurations 2(a) to 5(a), no decisive ferromagnetic phase stabilization occurs at room temperature, considering the electronic thermal fluctuation of the order of $k_B T$ as $\Delta E_{2(a)}$, $\Delta E_{3(a)}$, $\Delta E_{4(a)}$ and $\Delta E_{5(a)}$ are -3.1 meV/Co, 5.5 meV/Co, -44.7 meV/Co and 27.0 meV/Co respectively. Notable ferromagnetic phase stabilization occurs in configurations 6(a) and 7(a) where Co ions and H_I form Co- H_I -O-Co complexes as $\Delta E_{6(a)}$ and $\Delta E_{7(a)}$ are 124.9 meV/Co and 333.7 meV/Co respectively. The complex in configuration 6(a) with the maximum concentration and reasonable ferromagnetic phase stability is predicted to dominate the room temperature ferromagnetism in ZnO:Co with H_I , in contrast to antiferromagnetism in ZnO:Co in the absence of hydrogen shown by the same density functional calculations [Zhang *et al.*, 2009].

In configuration 1(b), Co ions are separated as far as possible while H_O is situated afar from both Co ions, representing a scattered pattern for the distribution of Co ions and H_O where none are nearest neighbours. When Co ions are nearest neighbour, they form a Co-O-Co complex within ab plane and along c direction while the H_O is located far away from the Co ions in configurations 2(b) and 3(b) respectively, and the H_O moves to the nearest neighbour to both Co ions in configurations 4(b) and 5(b) respectively.

The calculated formation energy, $E_{\text{Conf.No.}}^f$ and the difference in total energy between AFM and FM, $\Delta E_{\text{Conf.No.}}$ of $Zn_{14}Co_2O_{15}Ho$ in oxygen-poor environment versus configuration number are shown in Fig. 3. It clearly shows that $E_{1(b)}^f$ of 2.35 eV is the highest among other configurations followed by $E_{3(b)}^f$ and $E_{2(b)}^f$ of 2.28 eV and 2.24 eV respectively. These results show that slight stabilization is gained when Co ions aggregate as Co-O-Co complexes over the scattered configuration. Similar to the case of ZnO:Co with H_I , a strong aggregation tendency among Co ions and Ho exists. Configurations 4(b) and 5(b) are much further stabilized

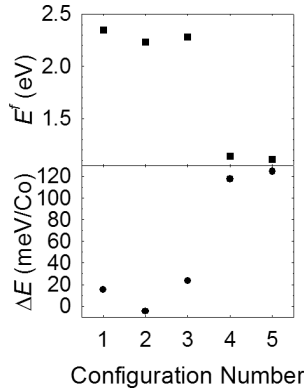


Fig. 3. (Top) Formation energy, $E_{\text{Conf.No.}}^f$ and (Bottom) difference in total energy between AFM and FM, $\Delta E_{\text{Conf.No.}}$ in configurations 1(b)–5(b) for $Zn_{14}Co_2O_{15}Ho$.

with $E_{4(b)}^f$ and $E_{5(b)}^f$ of 1.14 eV and 1.11 eV respectively, indicating that H_O tends to move into the O site between nearest neighbour Co ions. Configuration 5(b) is notably the most stable one, strongly suggesting a clustering tendency among Co ions and H_O to form a Co-Ho-Co complex. The relative concentration of complexes in configuration 5(b) over configuration 4(b) ($c_{5(b)}/c_{4(b)}$), the first and second most stable configurations, is 3 at room temperature. Clearly, configuration 5(b) is the dominant complex that consists of two Co ions and one H_O with the minimum possible separation in the ZnO supercell. However, all other complexes exhibit a small portion if present.

All configurations, excluding configurations 2(b), have ferromagnetic ground state. $\Delta E_{1(b)}$, $\Delta E_{2(b)}$ and $\Delta E_{3(b)}$ are 15.2 meV/Co, -4.6 meV/Co and 23.4 meV/Co respectively. The energy gained by ferromagnetic ordering in configurations 1(b) and 3(b), though positive, will not firmly confirm ferromagnetic coupling between Co ions at room temperature. Additionally, these complexes are unlikely to be present in thermodynamic equilibrium in comparison to the dominant configuration 5(b). As Co ions and Ho defect move closer to form Co-Ho-Co complexes, notable ferromagnetic phase stabilization occurs in configurations 4(b) and 5(b) as $\Delta E_{4(b)}$ and $\Delta E_{5(b)}$ are 117.6 meV/Co and 124.7 meV/Co respectively. The complex in configuration 5(b) with minimum formation energy and maximum ferromagnetic phase stability is predicted to dominate the room temperature ferromagnetism in ZnO:Co where Ho is present. The difference in formation energy was 0.4 eV between $E_{5(b)}^f$ and $E_{6(a)}^f$ as the most stable configurations of ZnO:Co are with H_I and Ho respectively which indicate that H_O is more stable in ZnO:Co. Considering this difference in formation energy, Ho is predicted to be the dominant form of hydrogen in ZnO:Co under oxygen-poor conditions.

4. Conclusion

In summary, total energy density functional calculations have demonstrated that: (i) Co ions have a strong tendency toward aggregation which is independent of the presence of H_I (Ho) in ZnO; (ii) When a high concentration of H_I (Ho) exists in ZnO:Co, the Co dopants and H_I (Ho) are arranged in complexes with very strong ferromagnetic signature that leads to the room temperature ferromagnetism, in contrast to antiferromagnetic coupling for Co ions in ZnO without hydrogen; (iii) In oxygen-poor environments, the formation of Ho in ZnO:Co is favored over H_I by 0.4 eV.

Acknowledgment

This work was supported by the Australia Research Council (ARC DP0770424).

References

Assadi, M. H. N., Zhang, Y. B. and Li, S. [2009] "Subtle interplay between native point defects and magnetism in ZnO:Co," *Appl. Phys. Lett.* **95**, 072503.

- Chambers, S. A., Droubay, T. C., Wang, C. M., Rosso, K. M., Heald, S. M., Schwartz, D. A., Kittilstved, K. R. and Gamelin, D. R. [2006] "Ferromagnetism in oxide semiconductors," *Mater. Today* **9**, 28–35.
- Janotti, A. and Van de Walle, C. G. [2007] "Hydrogen multicentre bonds," *Nat. Mater.* **6**, 44–47.
- Kaspar, T. C., Droubay, T., Heald, S. M., Nachimuthu, P., Wang, C. M., Shutthanandan, V., Johnson, C. A., Gamelin, D. R. and Chambers, S. A. [2008] "Lack of ferromagnetism in *n*-type cobalt-doped ZnO epitaxial thin films," *New J. Phys.* **10**, 055010.
- Pan, F., Song, C., Liu, X. J., Yang, Y. C. and Zeng, F. [2008] "Ferromagnetism and possible application in spintronics of transition-metal-doped ZnO films," *Mater. Sci. and Eng. R* **62**, 1–35.
- Park, C. H. and Chadi, D. J. [2005] "Hydrogen-mediated spin-spin interaction in ZnCoO," *Phys. Rev. Lett.* **94**, 127204.
- Prellier, W., Fouchet, A. and Mercey, B. [2003] "Oxide-diluted magnetic semiconductors: A review of the experimental status," *J. Phys.: Condens. Matter* **15**, R1583–R1601.
- Segall, M. D., Lindan, P. J. D., Probert, M. J., Pickard, C. J., Hasnip, P. J., Clark, S. J. and Payne, M. C. [2002] "First-principles simulation: Ideas, illustrations and the CASTEP code," *J. Phys.: Condens. Matter* **14**, 2717–2744.
- Van de Walle, C. G. [2000] "Hydrogen as a cause of doping in zinc oxide," *Phys. Rev. Lett.* **85**, 1012–1015.
- Van de Walle, C. G. and Neugebauer, J. [2004] "First-principles calculations for defects and impurities: Application to III-nitrides," *J. Appl. Phys.* **95**, 3851–3879.
- Walsh, A., Da Silva, J. L. F. and Wei, S. H. [2008] "Theoretical description of carrier mediated magnetism in cobalt doped ZnO," *Phys. Rev. Lett.* **100**, 256401.
- Zhang, Y. B., Assadi, M. H. N. and Li, S. [2009] "Isolation and aggregation of substituent Co in ZnO:Co diluted magnetic semiconductors," *J. Phys.: Condens. Matter* **21**, 175802.